Online Research @ Cardiff

This is an Open Access document downloaded from ORCA, Cardiff University's institutional repository: https://orca.cardiff.ac.uk/id/eprint/141965/

This is the author's version of a work that was submitted to / accepted for publication.

Citation for final published version:

Wang, Yaoqiang, Zhu, Yachang, Zhang, Xiaoguang, Tian, Bing, Wang, Kewen and Liang, Jun ORCID: https://orcid.org/0000-0001-7511-449X 2021. Anti-disturbance sliding mode based deadbeat direct torque control for PMSM speed regulation system. IEEE Transactions on Transportation Electrification 7 (4) , pp. 2705-2714. 10.1109/TTE.2021.3083074 file

Publishers page: http://dx.doi.org/10.1109/TTE.2021.3083074 <http://dx.doi.org/10.1109/TTE.2021.3083074>

Please note:
Changes made as a result of publishing processes such as copy-editing, formatting and page numbers may not be reflected in this version. For the definitive version of this publication, please refer to the published source. You are advised to consult the publisher's version if you wish to cite this paper.

This version is being made available in accordance with publisher policies. See http://orca.cf.ac.uk/policies.html for usage policies. Copyright and moral rights for publications made available in ORCA are retained by the copyright holders.

information services
gwasanaethau gwybodaeth

This article has been accepted for publication in a future issue of this journal, but has not been fully edited. Content may change prior to final publication. Citation information: DOI 10.1109/TTE.2021.3083074, IEEE Transactions on Transportation Electrification

Anti-disturbance Sliding Mode Based Deadbeat Direct Torque Control for PMSM Speed Regulation System

Yaoqiang Wang, *Senior Member*, *IEEE*, Yachang Zhu, Xiaoguang Zhang, *Member*, *IEEE*, Bing Tian, Kewen Wang, *Member*, *IEEE*, and Jun Liang, *Senior Member*, *IEEE*

Abstract—Deadbeat direct torque control (DBDTC) calculates the voltage vector based on the motor mathematical model and tracks the torque and flux reference within only one sampling cycle. However, in the traditional DBDTC, the reference torque is generated by a speed PI controller, which presents a low dynamic and poor precision, particularly under external disturbances. To sort out this issue, this paper proposes an improved DBDTC control method basing on the sliding mode strategy. First, an anti-disturbance sliding mode controller (ASMC) is presented which is superior in offering a fast and accurate reference torque for DBDTC. Along the way, an extended sliding mode disturbance observer is introduced which estimates total disturbances and compensates the sliding mode controller. To reduce the chattering of sliding mode control, a novel reaching law is proposed. This novel reaching law introduces system state variable in the exponential terms of power reaching law, and meanwhile including an adaptive exponential reaching action. By this means, it increases system convergence rate to the sliding mode surface while suppressing sliding mode chattering. Finally, both simulation and experimental results show that the proposed control method has better performance in terms of torque ripple reduction, speed dynamic response.

***Index Terms*—permanent magnet synchronous motor, deadbeat direct torque control, anti-disturbance sliding mode controller, novel reaching law.**

I. Introduction

DIRECT torque control (DTC) has been widely used in motor drives due to its simple structure and fast dynamic response [1]-[3]. However, the traditional direct torque control for a permanent magnet synchronous motor (PMSM) suffers the problems of, such as large torque and stator flux ripple, inconstant switching frequency, and poor performance at low speeds [4]-[6].

In this context, predictive control can be applied to fulfill the high-performance requirement of PMSM. Predictive torque control can be categorized into model predictive torque control (MPTC) [7]-[9], deadbeat direct torque control (DBDTC) [10]-[12]. Based on the discrete model of PMSM, MPTC optimizes the voltage vector to be applied through a cost function, however, the available voltage vectors can be quite limited. In other words, the model predictive torque control still suffers the problem of large torque ripples. Unlike MPTC, the voltage vectors of the deadbeat control to feed the motor is completely derived from the PMSM model and then transformed into a switching signal by pulse width modulation (PWM) techniques. In DBDTC, motor torque and stator flux are directly controlled, and the idea behind is to track torque and flux within one control cycle. Therefore, DBDTC has the advantages of a fixed switching frequency, small torque ripple, and fast dynamic response.

In recent years, DBDTC for PMSM has been widely studied [13]-[16]. In [13], a flux observer with a low sampling frequency in combination with a volt-second-based torque inverse model is proposed, which claims to improve the performance of DBDTC under a low switching frequency. In [14], the presented method switches between two different deadbeat controllers depending on a quantized torque regulation error. The dynamic and steady performance of the motor are improved, however, this method can be quite laborious to use. In [15], stator current and flux observers are proposed to improve the performance of DBDTC, however, the influence of inductance and resistance is overlooked. In [16], the DBDTC is introduced to optimize the voltage vector choices for a model predictive torque controller, which reduces not only the fluctuation of electromagnetic torque and stator flux but also the calculational burden of the MPTC.

In the traditional DBDTC, the reference torque is usually generated by speed PI controller. However, when the load torque variation and internal parameter perturbation occur, the control performance of PI controller is unsatisfactory. Sliding mode control (SMC) is a preferable selection because of its insensitivity to certain external disturbances and parameter

This work was supported in part by the National Natural Science Foundation of China under Grant 51507155, and in part by the Youth Key Teacher Project of Henan Higher Educational Institutions under Grant 2019GGJS011. (Corresponding author: Xiaoguang Zhang.)

Y. Wang and K. Wang are with the School of Electrical Engineering, Zhengzhou University, Zhengzhou 450001, China, and also with the Henan Engineering Research Center of Power Electronics and Energy Systems, Zhengzhou 450001, China (e-mail: WangyqEE@163.com, kwwang@zzu.edu.cn).

Y. Zhu is with Zhengzhou University, Zhengzhou 450001, China, and also with Yellow River Water Conservancy and Hydropower Development Group Co., Ltd, Zhengzhou 450001, China (e-mail: ZhuycEE@163.com).

X. Zhang is with the North China University of Technology, Beijing 100144, China (e-mail: zxg@ncut.edu.cn).

B. Tian is with the Nanjing University of Aeronautics and Astronautics, Nanjing 210000, China (e-mail: tianbing_hit@163.com.)

J. Liang is with Zhengzhou University, Zhengzhou 450001, China, and also with Cardiff University, Cardiff CF24 3AA, U.K. (e-mail: LiangJ1@cardiff.ac.uk).

2332-7782 (c) 2021 IEEE. Personal use is permitted, but republication/redistribution requires IEEE permission. See http://www.ieee.org/publications_standards/publications/rights/index.html for more information.
Authorized licensed use limited to: Zhengzhou University. Downloaded on May 25,2021 at 15:13:45 UTC from IEEE Xplore. Restrictions apply.

This article has been accepted for publication in a future issue of this journal, but has not been fully edited. Content may change prior to final publication. Citation information: DOI 10.1109/TTE.2021.3083074, IEEE Transactions on Transportation Electrification

perturbations as well as its robustness and fast response, and by far it has been successfully applied in advanced motor control fields [17]-[19]. SMC contains discontinuous control term, which makes the system have highly robust and can overcome the external disturbance and internal parameter perturbation imposed on the system. However, it also causes chattering of the control system[20]. This problem can be solved by observing and compensating disturbance with disturbance observer. In [21], a disturbance observer is adopted to compensate for the unmodeled uncertainty of the existing speed controller, which improves the anti-disturbance capability and robustness of the MPTC system. In [22], a method combining an improved exponential reaching law and a disturbance observer is presented to compensate for the reference voltage variation caused by the motor parameter perturbation, which improves the system robustness against the parameter drift. In [23], the aforesaid method is applied to the converter, and the experimental results show that both the robustness and stability of the system have the potential to be improved.

Besides, the practical instance of SMC suggest that converging to the equilibrium point is difficult as the system states approach the sliding surface and start to slide. In this context, the SMC is supposed to switching between the boundaries of the sliding surface, which inevitably leads to some chattering [24]-[26]. Since the reaching law is closely related to the sliding surface reaching manner, the associated chattering has the potential to be suppressed by exploiting novel reaching laws. [27] first brought up several new reaching laws to reduce sliding mode chattering. In [28], the terminal attractor is added on the basis of a traditional reaching law to achieve a fast convergence rate while sliding along the sliding mode surface, however, it is overparameterized. In [29], an optimized constant rate reaching law is applied to the sliding mode observer for accurate speed estimation.

This paper investigates a sliding mode control-based DBDTC strategy for a PMSM drive. Firstly, the influence of the reference torque precision on DBDTC is analyzed, and a sliding mode speed controller is proposed to precisely generate the reference torque for the DBDTC. Regarding the external disturbances, an extended sliding mode disturbance observer (ESMDO) is designed to compensate the unmodeled uncertainty while implementing the presented sliding mode speed controller, and they form the anti-disturbance sliding mode controller (ASMC) of this work. Particularly, to further improve its performance, a novel reaching law is used in the ASMC-DBDTC, which is featured by a fast convergence rate and proved competence to attenuate the chattering.

II. Design and Analysis of DBDTC

A. PMSM Mathematical Model

Under the synchronously rotating frame, the PMSM mathematical model can be expressed as

$$\begin{cases} u_d = Ri_d - \omega\psi_q + \dfrac{d\psi_d}{dt} \\ u_q = Ri_q + \omega\psi_d + \dfrac{d\psi_q}{dt} \end{cases} \tag{1}$$

$$\begin{cases} \psi_d = L_d i_d + \psi_f \\ \psi_q = L_q i_q \end{cases} \tag{2}$$

$$T_e = \frac{3}{2} p\left[\psi_f i_q + (L_d - L_q) i_d i_q\right] \tag{3}$$

$$J\dot{\omega} = T_e - B\omega - T_L \tag{4}$$

where u_d, u_q and i_d, i_q represent the voltages and currents of *d*- and *q*- axes, respectively; *R* is stator resistance; L_d and L_q are *d*- and *q*-axes inductances, for surface-mounted PMSM there is L_d=L_q=*L*; ψ_d and ψ_q are *d*- and *q*- axes flux linkages; ψ_f is permanent Magnet flux linkage; ω is the angular velocity; *J* is the rotational inertia; and T_e and T_L represent, respectively, the electromagnetic and load torques.

B. Digital delay compensation

Due to the sample and hold effect as well as the PWM update delay, the motor terminal voltage always lags its reference by one or more control periods. In other words, for precise control of motor voltages, the application of *kth* instant voltage vector shall be advanced to (*k*+1)*th* or (*k*+2)*th* instants. Evidently, the use of *kth* instant voltage vector does not suffice any longer, particularly under a low sampling frequency. Thus, the delay compensation is quite necessary.

Substituting (2) into (1) and applying the forward Euler method, the discrete domain stator current model of PMSM can be expressed as

$$i_s^{k+1} = i_s^k + \frac{T_s}{L_s}(u_s^k - Ri_s^k - j\omega\psi_f e^{j\theta}) \tag{5}$$

where *k* represents the *k*th sampling instant; T_s represents the sampling period.

From (5), the predicted current i_s^{k+1} can be deduced from the voltage u_s^k and the feedback current i_s^k, and in this way, the aforesaid digital delay is offset by engaging i_s^{k+1} in the deadbeat control.

C. Reference Voltage Prediction

To offset the digital delay effect, the predicted current by (5) is used, instead of the currently sampled current, to predict the electromagnetic torque and flux linkage. This can be partially completed by substituting (2) into (1), and it yields

$$\begin{cases} \psi_d^{k+2} = u_d^{k+1}T_s + \psi_d^{k+1} + \omega T_s\psi_q^{k+1} - \dfrac{R_s T_s}{L_d}(\psi_d^{k+1} - \psi_f) \\ \psi_q^{k+2} = u_q^{k+1}T_s + \psi_q^{k+1} - \omega T_s\psi_d^{k+1} - \dfrac{R_s T_s}{L_q}\psi_q^{k+1} \end{cases} \tag{6}$$

In addition, since voltage drop of resistance is much smaller than stator voltage when motor operates stably, the item of resistance in (6) can be ignored. Then,the amplitude of the stator flux linkage can be expressed as

$$\begin{aligned} (\psi_s^{k+2})^2 = (\psi_d^{k+2})^2 + (\psi_q^{k+2})^2 &= (u_d^{k+1}T_s + \psi_d^{k+1} \\ &+ \omega T_s\psi_q^{k+1})^2 + (u_q^{k+1}T_s + \psi_q^{k+1} - \omega T_s\psi_d^{k+1})^2 \end{aligned} \tag{7}$$

where ψ_s is the stator flux linkage.

In DBDTC, the predicted flux linkage is supposed to follow

2332-7782 (c) 2021 IEEE. Personal use is permitted, but republication/redistribution requires IEEE permission. See http://www.ieee.org/publications_standards/publications/rights/index.html for more information.
Authorized licensed use limited to: Zhengzhou University. Downloaded on May 25,2021 at 15:13:45 UTC from IEEE Xplore. Restrictions apply.

This article has been accepted for publication in a future issue of this journal, but has not been fully edited. Content may change prior to final publication. Citation information: DOI 10.1109/TTE.2021.3083074, IEEE Transactions on Transportation Electrification

its reference within one sampling period, and thus, let $\psi_s^{k+2}=\psi_s^*$. ψ_s^* can be obtained as follows

$$\psi_s^*=\sqrt{\psi_f^2+L_q^2(\frac{2T_e^*}{3p\psi_f})}\,. \tag{8}$$

Substitute (2) into (3) and then take the time derivative of the torque, it yields

$$T_e^{k+2}-T_e^{k+1}=\frac{3p\psi_f}{2L_s}(\psi_q^{k+2}-\psi_q^{k+1})\,. \tag{9}$$

Afterward, substitute (6) into (9), it yields

$$u_q^{k+1}T_s=D \tag{10}$$

where $D=\frac{2L_q}{3p\psi_f}(T_e^{k+2}-T_e^{k+1})+\frac{R_sT_s\psi_q^{k+1}}{L_q}+\omega T_s\psi_d^{k+1}$.

Likewise, to track the reference torque within one sampling period, let $T_e^{k+2}=T_e^*$.

Combine (7) with (10), the reference voltage vector for DBDTC can be obtained as follows

$$\begin{cases} u_d^{k+1}=\dfrac{-X_1\pm\sqrt{X_1^2-X_2}}{T_s} \\ u_q^{k+1}=\dfrac{D}{T_s} \end{cases} \tag{11}$$

with $X_1=\psi_d^{k+1}+\omega T_s\psi_q^{k+1}$

$$X_2=D^2+2D(\psi_q^{k+1}-\omega T_s\psi_d^{k+1})-(\psi_s^*)^2+[(\psi_d^{k+1})^2+(\psi_q^{k+1})^2](\omega^2T_s^2+1)$$

The DBDTC block diagram is shown in Fig.1. i_d and i_q are obtained by rotation transformation of the sampled three-phase currents, and they are then used to compute ψ_d^{k+1}, ψ_q^{k+1}, T_e^{k+1}. The reference torque T_e^* is assigned by the speed controller, whereas the reference flux is calculated by (8). Then substitute the above variables into (11), the reference voltage vector is therefore obtained. The reference voltage in DBDTC is concerned with the torque and flux prediction, and thence, an accurate reference torque can play an important role in this process.

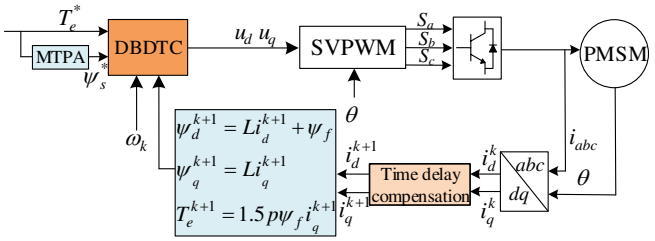

Fig. 1. Block diagram of DBDTC.

III. Proposed ASMC-DBDTC Scheme With Novel Reaching Law

According to the above analysis, the reference torque may affect the performance of DBDTC. The traditional DBDTC method uses the speed PI controller to generate the corresponding reference torque. However, when the load torque variation and internal parameter perturbation occur, the control performance of PI controller is unsatisfactory. Sliding mode control has shown the advantage of insensitivity to external disturbances and parameter perturbations as well as strong robustness and fast response, and thus, in this section an ASMC is proposed which is capable to quickly provide an accurate reference input for DBDTC. In addition, to further improve its performance, a novel reaching law is used in the ASMC-DBDTC, which is featured by a fast convergence rate and proved competence to attenuate the chattering.

A. Design of ESMDO

To compensate the impact of load disturbance and parameter perturbations, an extended sliding mode disturbance observer is used which is then merged with the presented sliding mode controller.

In the presence of parameter perturbations, (4) can be rewritten as

$$(J_0+\Delta J)\dot{\omega}=T_e-T_L-(B_0+\Delta B)\omega. \tag{12}$$

where J_0 and B_0 are the nominal values of the motor inertial and friction coefficient, and ΔJ and ΔB are the measured errors of motor parameters with respect to their nominal values.

Define r as the total disturbance which is represented by

$$r=-\Delta J\dot{\omega}-\Delta B\omega-T_L\,. \tag{13}$$

Then, (13) can be rewritten as

$$J_0\dot{\omega}=T_e-B_0\omega+r\,. \tag{14}$$

Regard r as an extended state variable, then an extended state equation is obtained and given by

$$\begin{bmatrix}\dot{\omega}\\ \dot{r}\end{bmatrix}=\begin{bmatrix}\frac{-B}{J} & \frac{1}{J}\\ 0 & 0\end{bmatrix}\begin{bmatrix}\omega\\ r\end{bmatrix}+\begin{bmatrix}\frac{1}{J}\\ 0\end{bmatrix}T_e \tag{15}$$

In the sliding-mode disturbance observer, the speed ω and total disturbance r act as the primary goals of observation, and hence, the following equation is constructed

$$\begin{bmatrix}\dot{\hat{\omega}}\\ \dot{\hat{r}}\end{bmatrix}=\begin{bmatrix}\frac{-B}{J} & \frac{1}{J}\\ 0 & 0\end{bmatrix}\begin{bmatrix}\hat{\omega}\\ \hat{r}\end{bmatrix}+\begin{bmatrix}\frac{1}{J}\\ 0\end{bmatrix}T_e+\begin{bmatrix}\frac{1}{J}\\ g\end{bmatrix}u_{smo} \tag{16}$$

where $\hat{r}$ is the estimated total disturbance, $\hat{\omega}$ is the estimated value of the speed, and g is the sliding mode coefficient, with the control law $u_{\rm smo}$ designed as

$$u_{smo}=\eta\cdot\mathrm{sgn}(s) \tag{17}$$

where η is negative and $S=\hat{\omega}-\omega$ is the preferred sliding-mode surface.

Subtracting (15) from (16) yields the state equation for estimation error

$$\begin{cases}\dot{e}_\omega=J_0^{-1}(-B_0e_\omega+e_r+u_{smo})\\ \dot{e}_r=gu_{smo}\end{cases} \tag{18}$$

where $e_\omega=\hat{\omega}-\omega$ and $e_r=\hat{r}-r$.

To guarantee the estimation error decreases over time, the preferences of sliding mode observer should meet

$$\begin{aligned}e_\omega\cdot\dot{e}_\omega&=J_0^{-1}e_\omega[-B_0e_\omega+e_r+u_{smo}]\\ &=J_0^{-1}e_\omega[-B_0e_\omega+e_r+\eta\,\mathrm{sgn}(e_\omega)]<0\end{aligned}\,. \tag{19}$$

2332-7782 (c) 2021 IEEE. Personal use is permitted, but republication/redistribution requires IEEE permission. See http://www.ieee.org/publications_standards/publications/rights/index.html for more information.
Authorized licensed use limited to: Zhengzhou University. Downloaded on May 25,2021 at 15:13:45 UTC from IEEE Xplore. Restrictions apply.

This article has been accepted for publication in a future issue of this journal, but has not been fully edited. Content may change prior to final publication. Citation information: DOI 10.1109/TTE.2021.3083074, IEEE Transactions on Transportation Electrification

Therefore, the coefficient η should satisfy

$$\eta < -\left|e_r - B_0 e_\omega\right|. \tag{20}$$

Once the observer reaches sliding-mode surface in a finite time, and stays on it, there is $e_\omega = \dot{e}_\omega = 0$. In this context, (18) can be simplified as

$$\begin{cases} e_r = -u_{smo} \\ \dot{e}_r = g u_{smo} \end{cases}. \tag{21}$$

Solve (21), one can have

$$e_r = ce^{-gt} \tag{22}$$

where c is a constant, positive.

From (22), to force the estimation error to converge to zero, the coefficient g needs to satisfy $g > 0$.

B. Anti-disturbance Sliding Mode Controller

The speed error is defined as the PMSM speed regulation system state variable:

$$x = \omega^* - \omega \tag{23}$$

where ω^* is the reference speed; ω is the actual speed.

Combine (14) with (23), the derivative of x can be expressed as

$$\dot{x} = -J_0^{-1}(T_e - B_0\omega + r) \tag{24}$$

where the total disturbance r which can be replaced by its estimate value $\hat{r}$.

An integral sliding mode surface is preferred which is shown as follows

$$s = x + c\int_0^t x d\tau \quad c > 0. \tag{25}$$

The traditional sliding mode control only concerns about the steady-state without taking care of the sliding process. To gain a better control performance, the sliding mode control law can use a power reaching law

$$\frac{ds}{dt} = -\varepsilon\left|s\right|^\lambda \operatorname{sgn}(s), \quad \varepsilon > 0, 0 < \lambda < 1 \tag{26}$$

where s is the sliding surface, λ is the exponent in the power function. When $s(0) > 0$ and $s(t) = 0$, the reaching time can be calculated by integrating (26) from 0 to t.

$$t = \frac{s(0)^{1-\lambda}}{\varepsilon(1-\lambda)}. \tag{27}$$

From (26) and (27), it can be known that the reaching speed is related to the choices of ε and λ. Increasing ε improves the reaching speed, however, it also increases the chattering; On the other hand, increasing λ also improves the system reaching speed when the initial error is far away from the sliding surface, but the convergence slows down remarkably when close to the sliding surface. Therefore, in practice, the parameters of the reaching law should be selected by taking care of both reaching speed and chattering level.

Combine (24) and (25) with (26), the reference torque can be obtained as

$$T_e^* = J_0[cx + \varepsilon\left|s\right|^\lambda \operatorname{sgn}(s)] + B_0\omega - \hat{r}. \tag{28}$$

C. Proposed Novel Reaching Law

Although the power reaching law is able to reach the sliding mode surface within a limited time, it suffers a slow reaching speed and long reaching time when the system initial state is far away from the sliding mode surface, which limits its practical value. To circumvent this shortcoming, this paper proposes a novel reaching law on the basis of the power reaching law, which is expressed as

$$\begin{aligned} &\frac{ds}{dt} = -\varepsilon\left|s\right|^\delta \operatorname{sgn}(s) - k\left|x\right|^\gamma s, \quad \delta = \alpha + (\lambda - \alpha)e^{-\beta|x|} \\ &\lim_{t\to\infty}\left|x\right| = 0, \varepsilon > 0, k > 0, \alpha > 1, 0 < \lambda < 1, \beta > 0, \gamma > 1 \end{aligned} \tag{29}$$

where s is the sliding mode surface and x is the system state variable.

As revealed by (29), the novel reaching law introduces a state variable $|x|$ to control the convergence rate, where the exponent of $|s|$ can vary along with x now and it forms a variable power exponential power reaching law with the last term corresponding to an adaptive exponential reaching law. The following conclusions can be deduced: When the system initial state is far away from the sliding surface, i.e., $|x|$ is relatively large and δ approaches α, and in this case, the system state will be driven onto the sliding surface swiftly attributed to the actions of both $-\varepsilon|s|^\delta\operatorname{sgn}(s)$ and $-k|x|^\gamma s$, and hence, it solves the problem of long reaching time in the traditional power reaching law. As the system state approaches the sliding mode surface, $|x|$ converges to zero and the exponent of $|s|$ approaches λ, meanwhile, the adaptive exponential term is almost null. In this process, only $-\varepsilon|s|^\delta\operatorname{sgn}(s)$ is practically engaged, resulting in a small chattering while sliding along the sliding mode surface.

From (29), δ=1 divides the reaching event into, respectively, the fast convergence and sliding mode motion phases, and plugging this value into (29), it obtains

$$\left|x_0\right| = \frac{1}{\beta}\ln\frac{\alpha - \lambda}{\alpha - 1}. \tag{30}$$

where x_0 denotes this division point. As a summary, the system state reaches the sliding mode surface quickly when δ>1 and slides along the surface when δ<1, which retains the advantages of the traditional power rate reaching law with restrained chattering.

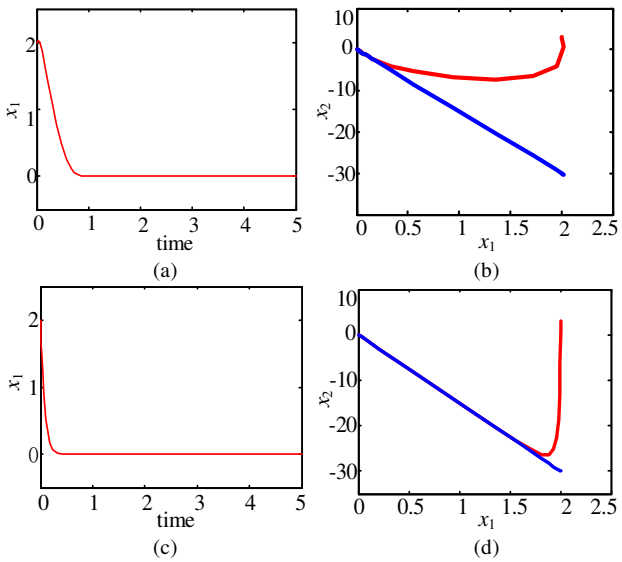

Fig. 2. Reaching behavior contrasts between power reaching law and novel reaching law. (a) convergence rate under the power reaching law. (b) Phase trajectory of power reaching law. (c) convergence rate under novel reaching law. (d) Phase trajectory of novel reaching law.

2332-7782 (c) 2021 IEEE. Personal use is permitted, but republication/redistribution requires IEEE permission. See http://www.ieee.org/publications_standards/publications/rights/index.html for more information.
Authorized licensed use limited to: Zhengzhou University. Downloaded on May 25,2021 at 15:13:45 UTC from IEEE Xplore. Restrictions apply.

This article has been accepted for publication in a future issue of this journal, but has not been fully edited. Content may change prior to final publication. Citation information: DOI 10.1109/TTE.2021.3083074, IEEE Transactions on Transportation Electrification

D. Performance Analysis of Novel Reaching Law

In this section, the reaching speed and chattering level of the aforesaid two reaching laws are analyzed. To facilitate the contrast, a universal state equation is established below

$$\frac{dx}{dt} = Ax + Fu \,. \tag{31}$$

Define the sliding surface s=Cx and its derivative can be expressed as follows

$$\frac{ds}{dt} = C\frac{dx}{dt} \,. \tag{32}$$

Substitute (29) and (31) into (32), it results in the following sliding mode control law

$$u = (CF)^{-1}[-CAx - \varepsilon |s|^{\alpha+(\lambda-\alpha)e^{-\beta|s|}} - k|x|^{\gamma} s] \tag{33}$$

where x=[x_1,x_2]$^{\mathrm{T}}$, x_1, x_2 are system state variables.

As a case study, assume $A = \begin{bmatrix} 0 & 1 \\ 0 & -25 \end{bmatrix}$, $F = \begin{bmatrix} 0 \\ 133 \end{bmatrix}$, $C = \begin{bmatrix} 15 & 1 \end{bmatrix}$, and the initial state $x(0)$=[-2,-2] with ε=15, k=10, a=1.5, λ=β=0.5, γ=2.

The simulations of, respectively, the novel reaching law and the traditional power reaching law using the same preferences are depicted in Fig.2. Evidently, the system convergence rate is faster under the novel reaching law, which means that when the system is disturbed, it can return to the steady state faster.

When the sliding-mode surface is close to 0，the novel reaching law can be simplified as

$$\frac{ds}{dt} = \varepsilon |s|^{\delta} \operatorname{sgn}(s(n)), \delta = \alpha + (\lambda - \alpha)e^{-\beta|x|} \,. \tag{34}$$

To analyze the chattering level of the novel reaching law, (34) is discretized as

$$s(n+1) - s(n) = -\varepsilon T |x|^{\delta} \operatorname{sgn}(s(n)) \tag{35}$$

where T is the sampling period.

Assume the system state reaches the sliding mode surface from an initial state of, respectively, s>0 and s<0, *i.e.*, $s(n)$=0$^+$ and $s(n)$=0$^-$.

Then, s of the next period, in the case of $s(n)$=0$^+$, can be updated as:

$$s(n+1) = -\varepsilon T |x|^{\delta} \,. \tag{36}$$

And s of the next period, in the case of $s(n)$=0$^-$, is given by

$$s(n+1) = \varepsilon T |x|^{\delta} \,. \tag{37}$$

According to (36) and (37), the switching boundary width of the discrete novel reaching law is

$$\zeta = 2\varepsilon T |x|^{\delta} \,. \tag{38}$$

Following an analogous principle, the switching boundary width of the traditional discrete power reaching law is denoted as

$$\zeta_1 = 2\varepsilon T |x|^{\lambda} \,. \tag{39}$$

Since the condition $\delta \geq \lambda$ is always fulfilled, one can have $\zeta \leq \zeta_1$, which suggests that chattering can be restrained under the novel reaching law.

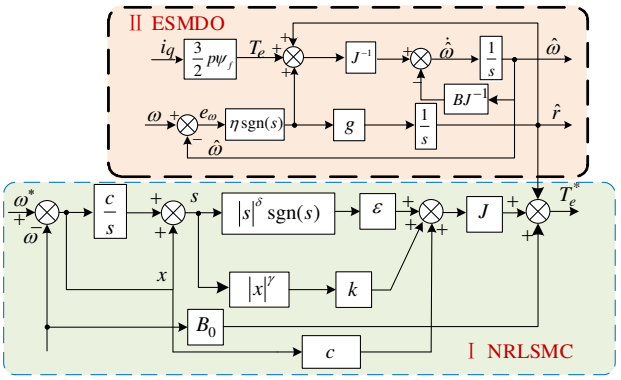

Fig. 3. Block diagram of NASMC.

E. Design of ASMC Based on Novel Reaching Law

To further improve the performance of DBDTC, an anti-disturbance sliding mode controller in conjunction with the novel reaching law (i.e., NASMC in this work) is presented as a replacement over ASMC.

Substitute (24) and (25) into (29), the reference torque can be rewritten as

$$T_e^* = J_0[cx + \varepsilon |s|^{\delta} \operatorname{sgn}(s) + k|x|^{\gamma} s] + B_0\omega - \hat{r} \,. \tag{40}$$

where c, ε, k are constants, $x = \omega^* - \omega$, s is the sliding surface, $\hat{r}$ is the estimated total disturbance.

The block diagram of NASMC is shown in Fig. 3, which consists of a sliding mode controller represented by Equation (40) and an extended sliding mode disturbance observer represented by Equation (16). It is expected that the total disturbance of the system will be compensated to the sliding mode controller by ESMDO to improve the control accuracy.

In order to verify the stability of the control method NASMC, the Lyapunov theory is applied where the Lyapunov function is chosen as $V = s^2/2$. According to (24), (25), and (40), the following relations can be obtained

$$\begin{aligned} \dot{V} = s\dot{s} &= s[-J_0^{-1}(T_e^* - B_0\omega + r) + cx] \\ &= s[-\varepsilon |s|^{\delta} \operatorname{sgn}(s) - k|x|^{\gamma} s] \leq 0 \end{aligned} \,. \tag{41}$$

Evidently, the designed control system satisfies the stability requirement, and this means the tracking error will converge to zero in a finite time.

IV. Simulation And Experimental Results

To confirm the validity of the presented NASMC-DBDTC method, comparative studies with the former methods, i.e., PI-DBDTC, ASMC-DBDTC are carried out via simulation and experiment. The motor parameters used for the simulation and the laboratory test rig are shown in Table I.

TABLE I
Parameters Of The Motor

Parameters and units	Values
Rated power P_n/kW	0.4
Inductance L_d = L_q/mH	6.71
Flux linkage of permanent magnets ψ_a/Wb	0.175
Stator phase resistance R/Ω	1.55
Viscous friction coefficient B/N·m·s	0.000 3
Rotational inertia J/kg·m^2	0.000 2

2332-7782 (c) 2021 IEEE. Personal use is permitted, but republication/redistribution requires IEEE permission. See http://www.ieee.org/publications_standards/publications/rights/index.html for more information.
Authorized licensed use limited to: Zhengzhou University. Downloaded on May 25,2021 at 15:13:45 UTC from IEEE Xplore. Restrictions apply.

This article has been accepted for publication in a future issue of this journal, but has not been fully edited. Content may change prior to final publication. Citation information: DOI 10.1109/TTE.2021.3083074, IEEE Transactions on Transportation Electrification

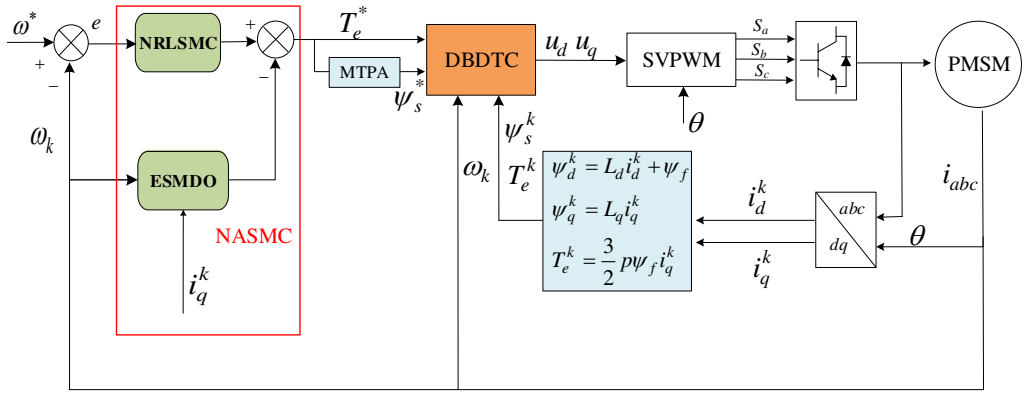

Fig. 4. Block diagram of NASMC-DBDTC method.

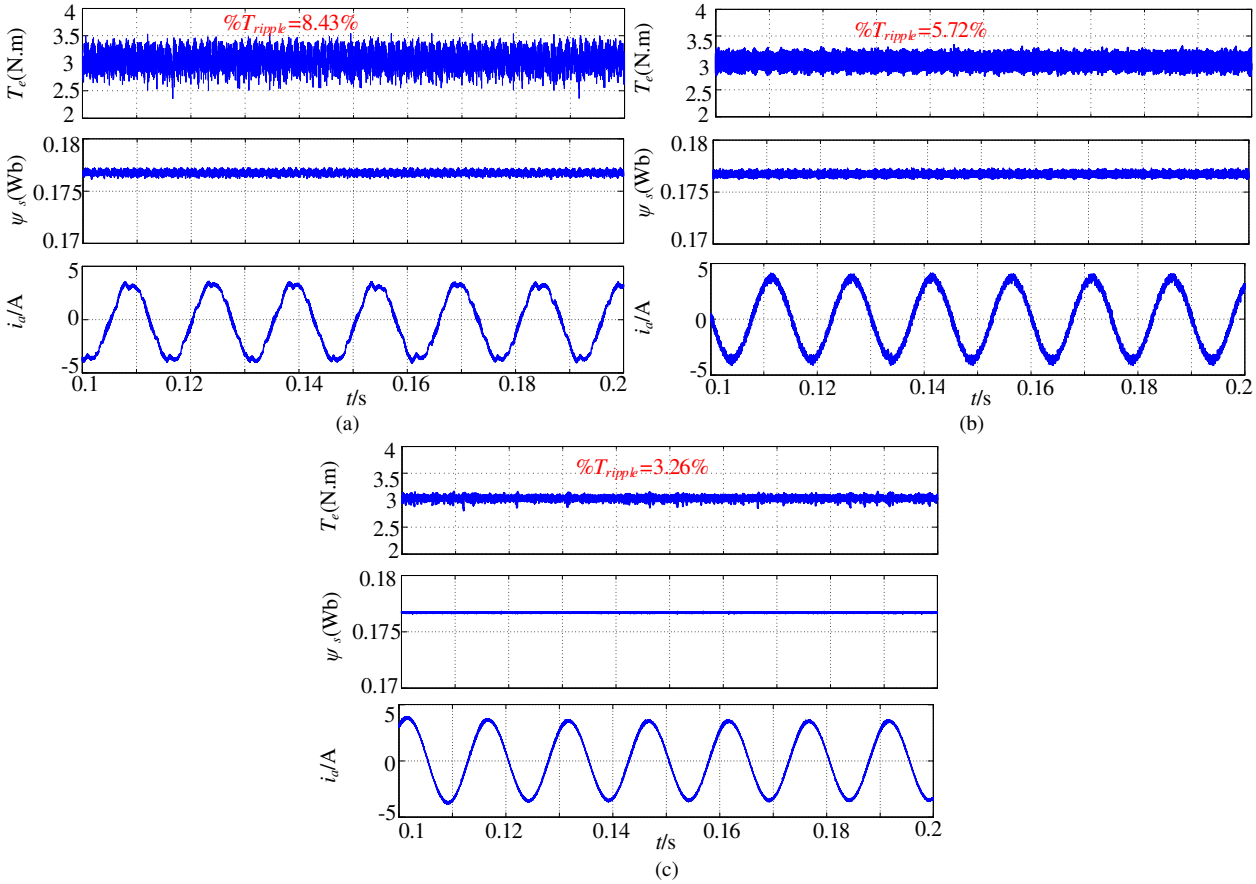

Fig. 5. Steady state results under. (a) PI-DBDTC method. (b) ASMC-DBDTC method. (c) NASMC-DBDTC method.

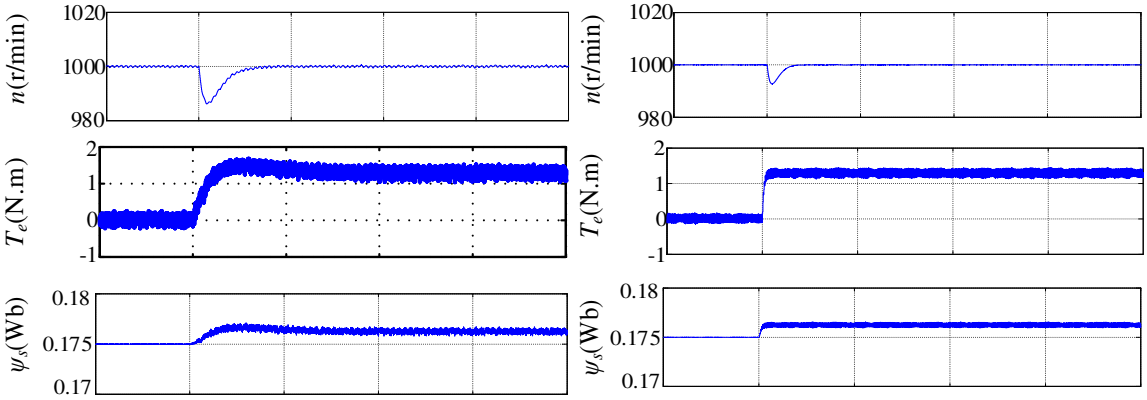

2332-7782 (c) 2021 IEEE. Personal use is permitted, but republication/redistribution requires IEEE permission. See http://www.ieee.org/publications_standards/publications/rights/index.html for more information.
Authorized licensed use limited to: Zhengzhou University. Downloaded on May 25,2021 at 15:13:45 UTC from IEEE Xplore. Restrictions apply.

This article has been accepted for publication in a future issue of this journal, but has not been fully edited. Content may change prior to final publication. Citation information: DOI 10.1109/TTE.2021.3083074, IEEE Transactions on Transportation Electrification

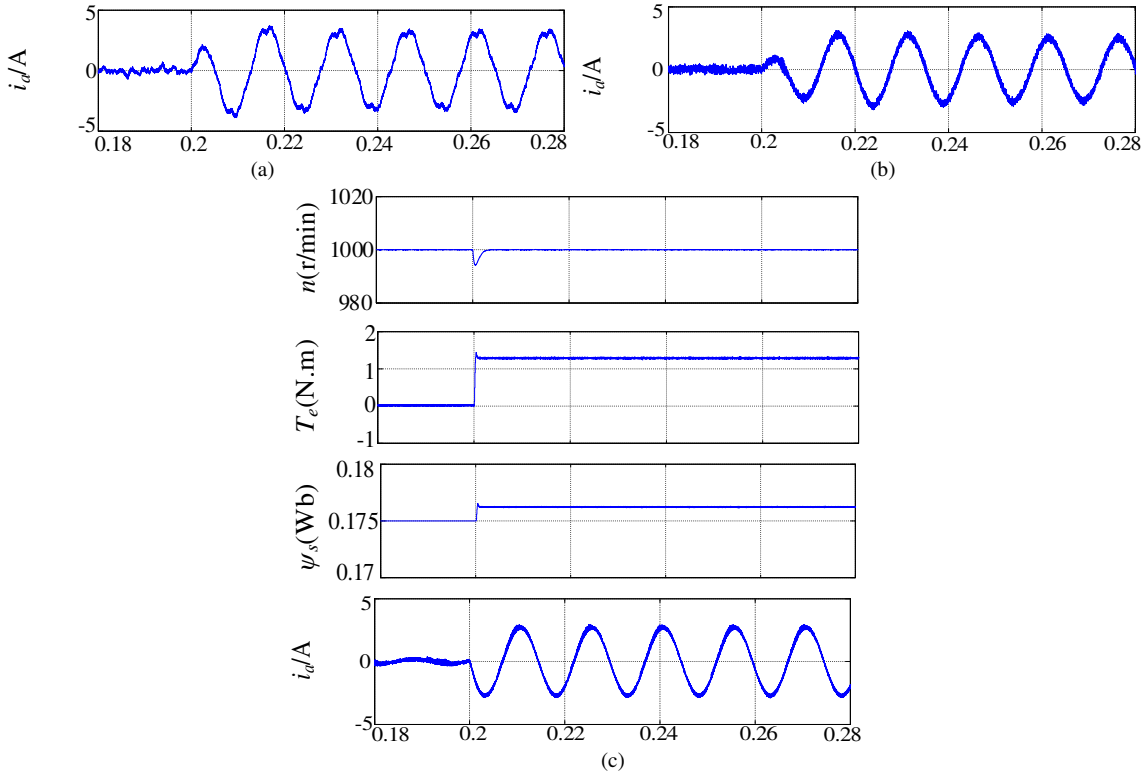

Fig. 6. Dynamic performance under. (a) PI-DBDTC method. (b) ASMC-DBDTC method. (c) NASMC-DBDTC method.

A. *Simulation Verification*

The control block diagram of PMSM drives is shown in Fig.4, where the ASMC controller is used to replace the PI controller to provide a fast and accurate reference torque for the next layer DBDTC.

The electromagnetic torque ripple is defined as

$$\begin{cases} T_{ripple} = \sqrt{\dfrac{1}{n}\sum_{i=1}^{n}\left(T_e(i) - T_{e\_ave}\right)^2} \\ \%T_{ripple} = \dfrac{T_{ripple}}{T_{e\_ave}} \times 100\% \end{cases} \tag{42}$$

Fig.5 demonstrates the steady-state performance of these three methods at 1000 r/min under a 3N•m load torque. It can be seen from Fig.5 (a) that the torque ripple of the PI-DBDTC method is 8.43%. In ASMC-DBDTC method, the torque ripple is reduced to 5.72%, however, the current waveform is still not that smooth with amounts of chattering. In the case of NASMC-DBDTC method, the torque ripple is further reduced owing to the novel reaching law, and the current waveform is much smoother, which confirms the validity of the presented novel reaching law in suppressing the chattering.

The dynamic performance is also evaluated as shown in Fig.6. In the simulation, the motor is rotated to 1000 r/min with no load, then a load torque of 1.27N•m is suddenly exerted on the shaft at 0.2s. From the simulation results, it can be seen that after the load variation, the torque response time of PI-DBDTC is 20ms, the speed fluctuation is 18 r/min, and the speed dynamic setting time is 10ms. The ASMC-DBDTC outperforms the PI-DBDTC in terms of fast torque response, small speed fluctuation, and fast recovery to the steady state. However, when contrasting Figs.6(b) and (c), it is visible that the NASMC-DBDTC method is superior in the dynamic behaviors and torque ripples, attributed to the novel reaching law.

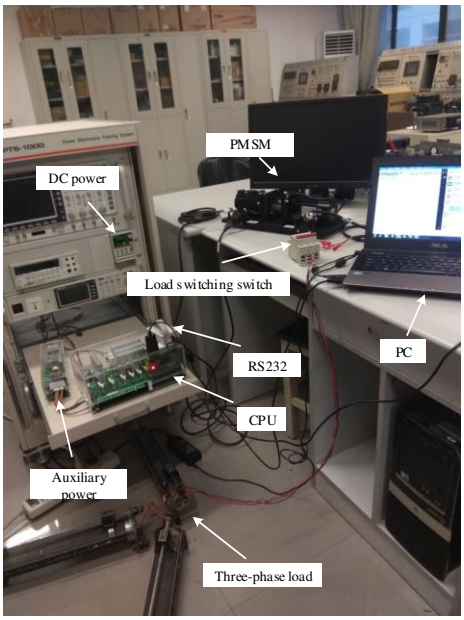

Fig. 7. Experimental hardware platform.

B. *Experimental Verification*

To further confirm the superiority of the proposed method, the aforesaid three methods are comparatively investigated via experiment. In the experiment, the control performance is judged from the starting time of the motor to a given speed, and the motor speed fluctuation, the dynamic setting time

2332-7782 (c) 2021 IEEE. Personal use is permitted, but republication/redistribution requires IEEE permission. See http://www.ieee.org/publications_standards/publications/rights/index.html for more information.
Authorized licensed use limited to: Zhengzhou University. Downloaded on May 25,2021 at 15:13:45 UTC from IEEE Xplore. Restrictions apply.

This article has been accepted for publication in a future issue of this journal, but has not been fully edited. Content may change prior to final publication. Citation information: DOI 10.1109/TTE.2021.3083074, IEEE Transactions on Transportation Electrification

when the load torque variations occurs. The shorter the starting time is, the smaller the speed fluctuation is, the faster the dynamic setting time is, which means the better the dynamic performance is. The experiment hardware platform is shown in Fig.7. The experimental motor parameters are as follows: rated power 0.4kW, bus voltage 110V, rated current 2.6A, rated speed 3000 r/min.

First of all, the startup performance is experimentally examined. For this purpose, the motor is started up to 1000 r/min with no load using the three control schemes (i.e., PI-DBDTC, ASMC-DBDTC, NASMC-DBDTC, respectively). From Fig.8, when the PI-DBDTC method is engaged, the speed experiences an overshoot of 50 rpm and the dynamic settling time is 220ms which is longer than 110ms that of the ASMC-DBDTC method. In contrast, the NASMC-DBDTC method has no overshoot in the speed profile and the settling time is only 80ms which reduces the settling time by 27%.

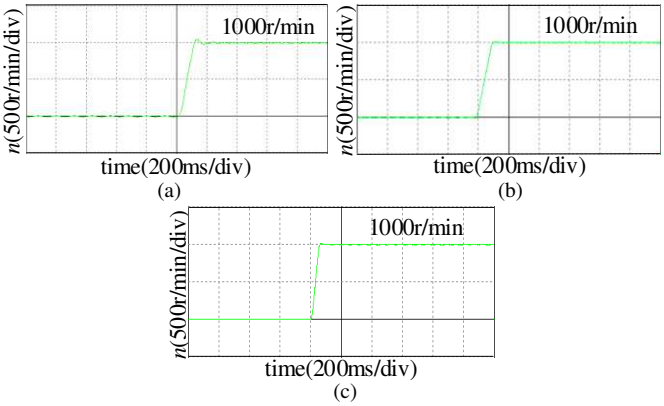

Fig. 8. Startup experiment contrast under three methods. (a) PI-DBDTC method. (b) ASMC-DBDTC method. (c) NASMC-DBDTC method.

Fig.9 shows the steady-state currents of three different methods under the rated load conditions. From the figure, the current ripple of PI-DBDTC is evidently large while in the ASMC-DBDTC case the ripple is reduced a bit but still larger than that in the NASMC-DBDTC case. This test demonstrates the presented novel reaching law outperforms in restraining the chattering.

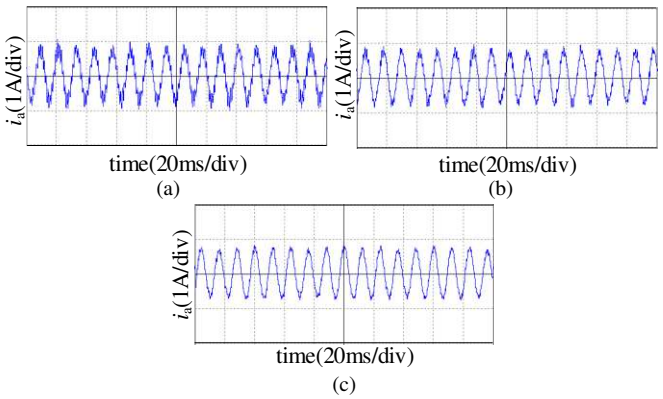

Fig. 9. Steady-state current waveform under three methods. (a) PI-DBDTC method. (b) ASMC-DBDTC method. (c) NASMC-DBDTC method.

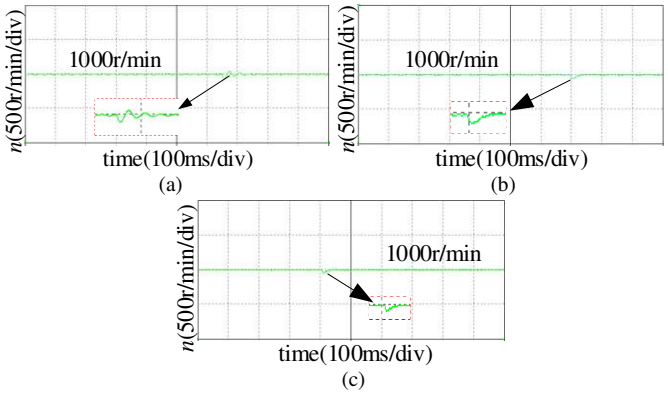

Fig. 10. Dynamic response experimental results under a varying load torque. (a) PI-DBDTC method. (b) ASMC-DBDTC method. (c) NASMC-DBDTC method.

The experiments in response to external disturbance are also conducted to further evaluate the anti-disturbance performance. In this test, an additional load torque of 1.27N·m is abruptly imposed at a certain instant of the steady-state. As can be known from Fig.10, after the load torque disturbance at a speed of 1000 r/min, a speed overshoot and its subsequent oscillation are notable in the PI-DBDTC method, with the dynamic settling time about 150ms. In contrast, both ASMC-DBDTC and NASMC-DBDTC presents a quickly damped oscillation in response to this disturbance and the proposed NASMC-DBDTC is more efficient. In addition, it can be seen that the speed fluctuation of NASMC-DBDTC method under a sudden load variation is smaller than other two control methods, indicating that it has better anti-disturbance ability.

V. Conclusion

A sliding mode control along with a disturbance observer is presented to improve the speed dynamic of a DBDTC-based PMSM drive. Two advanced reaching laws are introduced, i.e., the power reaching law and its upgraded version (termed the novel reaching law in this work). The SMCs using both reaching laws are capable to provide a quick and accurate reference input for the inner-layer DBDTC, with a decent immunity to the external disturbances, however, the proposed NASMC-DBDTC using the novel reaching law is more efficient in terms of dynamic performance and the steady-state chattering level. Comparisons among PI-DBDTC as well as ASMC-DBDTC and NASMC-DBDTC are carried out via the simulation and experiment, and the superiority of the proposed NASMC-DBDTC is confirmed.

References

[1] G. S. Buja and M. P. Kazmierkowski, "Direct torque control of PWM inverter-fed AC motors - a survey," in IEEE Transactions on Industrial Electronics, vol. 51, no. 4, pp. 744-757, Aug. 2004.

[2] A. Abosh, Z. Zhu, and Y. Ren, "Reduction of torque and flux ripples in space-vector modulation based direct torque control of asymmetric permanent magnet synchronous machine," in IEEE Transactions on Power Electronics, vol. 32, no. 4, pp. 2976–2986, Apr. 2016.

[3] C. Xia, S. Wang, X. Gu, Y. Yan and T. Shi, "Direct Torque Control for VSI-PMSM Using Vector Evaluation Factor Table," in IEEE Transactions on Industrial Electronics, vol. 63, no. 7, pp. 4571-4583, July. 2016.

[4] Y. Ren, Z. Q. Zhu and J. Liu, "Direct Torque Control of Perma-

2332-7782 (c) 2021 IEEE. Personal use is permitted, but republication/redistribution requires IEEE permission. See http://www.ieee.org/publications_standards/publications/rights/index.html for more information.
Authorized licensed use limited to: Zhengzhou University. Downloaded on May 25,2021 at 15:13:45 UTC from IEEE Xplore. Restrictions apply.

This article has been accepted for publication in a future issue of this journal, but has not been fully edited. Content may change prior to final publication. Citation information: DOI 10.1109/TTE.2021.3083074, IEEE Transactions on Transportation Electrification

nent-Magnet Synchronous Machine Drives With a Simple Duty Ratio Regulator," in IEEE Transactions on Industrial Electronics, vol. 61, no. 10, pp. 5249-5258, Oct. 2014

[5] D. Casadei, G. Serra and K. Tani, "Implementation of a direct control algorithm for induction motors based on discrete space vector modulation," in IEEE Transactions on Power Electronics, vol. 15, no. 4, pp. 769-777, July. 2000.

[6] F. Niu, K. Li, and Y. Wang, "Direct torque control for permanent magnet synchronous machines based on duty ratio modulation," in IEEE Transactions on Power Electronics, vol. 62, no. 10, pp. 6160–6170, Oct. 2015.

[7] T. Geyer, G. Papafotiou, and M. Morari, "Model predictive direct torque Control–Part I: Concept, algorithm, and analysis," in IEEE Transactions on Industrial Electronics, vol. 56, no. 6, pp. 1894–1905, Jun. 2009.

[8] P. Correa, M. Pacas, and J. Rodriguez, "Predictive torque control for inverter-fed induction machines," in IEEE Transactions on Industrial Electronics., vol. 54, no. 2, pp. 1073–1079, Apr. 2007

[9] W. Xie et al., "Finite-control-set model predictive torque control with a deadbeat solution for PMSM drives," in IEEE Transactions on Industrial Electronics, vol. 62, no. 9, pp. 5402–5410, Sep. 2015.

[10] A. D. Alexandrou, N. K. Adamopoulos and A. G. Kladas, "Development of a Constant Switching Frequency Deadbeat Predictive Control Technique for Field-Oriented Synchronous Permanent-Magnet Motor Drive," in IEEE Transactions on Industrial Electronics, vol. 63, no. 8, pp. 5167-5175, Aug. 2016.

[11] J. S. Lee, R. D. Lorenz and M. A. Valenzuela, "Time-Optimal and Loss-Minimizing Deadbeat-Direct Torque and Flux Control for Interior Permanent-Magnet Synchronous Machines," in IEEE Transactions on Industry Applications, vol. 50, no. 3, pp. 1880-1890, May-June 2014.

[12] M. Saur, D. E. Gaona Erazo, J. Zdravkovic, B. Lehner, D. Gerling and R. D. Lorenz, "Minimizing Torque Ripple of Highly Saturated Salient Pole Synchronous Machines by Applying DB-DTFC," in IEEE Transactions on Industry Applications, vol. 53, no. 4, pp. 3643-3651, July-Aug 2017.

[13] Y. Wang, S. Tobayashi and R. D. Lorenz, "A Low-Switching-Frequency Flux Observer and Torque Model of Deadbeat–Direct Torque and Flux Control on Induction Machine Drives," in IEEE Transactions on Industry Applications, vol. 51, no. 3, pp. 2255-2267, May-June 2015.

[14] M. H. Vafaie, B. M. Dehkordi, P. Moallem and A. Kiyoumarsi, "Improving the Steady-State and Transient-State Performances of PMSM Through an Advanced Deadbeat Direct Torque and Flux Control System," in IEEE Transactions on Power Electronics, vol. 32, no. 4, pp. 2964-2975, April. 2017.

[15] J. S. Lee, C. Choi, J.-K. Seok, and R. D. Lorenz, "Deadbeat-direct torque and flux control of interior permanent magnet synchronous machines with discrete time stator current and stator flux linkage observer," in IEEE Transactions on Industry Applications, vol. 47, no. 4, pp. 1749–1758, Jul-Aug 2011.

[16] X. Zhang and B. Hou, "Double Vectors Model Predictive Torque Control Without Weighting Factor Based on Voltage Tracking Error," in IEEE Transactions on Power Electronics, vol. 33, no. 3, pp. 2368-2380, March. 2018.

[17] V. Repecho, D. Biel and A. Arias, "Fixed Switching Period Discrete-Time Sliding Mode Current Control of a PMSM," in IEEE Transactions on Industrial Electronics, vol. 65, no. 3, pp. 2039-2048, March.2018.

[18] Y. Feng, X. Yu and F. Han, "High-Order Terminal Sliding-Mode Observer for Parameter Estimation of a Permanent-Magnet Synchronous Motor," in IEEE Transactions on Industrial Electronics, vol. 60, no. 10, pp. 4272-4280, Oct. 2013.

[19] Y. Wang, Y. Feng, X. Zhang and J. Liang, "A New Reaching Law for Antidisturbance Sliding-Mode Control of PMSM Speed Regulation System," in IEEE Transactions on Power Electronics, vol. 35, no. 4, pp. 4117-4126, April. 2020.

[20] X. Zhang, L. Sun, K. Zhao and L. Sun, "Nonlinear Speed Control for PMSM System Using Sliding-Mode Control and Disturbance Compensation Techniques," in IEEE Transactions on Power Electronics, vol.28, no. 3, pp. 1358-1365, March. 2013.

[21] J. Wang, F. Wang, Z. Zhang, S. Li and J. Rodríguez, "Design and Implementation of Disturbance Compensation-Based Enhanced Robust Finite Control Set Predictive Torque Control for Induction Motor Systems," in IEEE Transactions on Industrial Informatics, vol. 13, no. 5, pp. 2645-2656, Oct. 2017.

[22] X. Zhang, B. Hou and Y. Mei, "Deadbeat Predictive Current Control of Permanent-Magnet Synchronous Motors with Stator Current and Disturbance Observer," in IEEE Transactions on Power Electronics, vol. 32, no. 5, pp. 3818-3834, May. 2017.

[23] Y. Wu and Y. Ye, "Internal Model-Based Disturbance Observer With Application to CVCF PWM Inverter," in IEEE Transactions on Industrial Electronics, vol. 65, no. 7, pp. 5743-5753, July. 2018.

[24] Sabanovic, "Variable Structure Systems With Sliding-modes in Motion Control—A Survey," in IEEE Transactions on Industrial Informatics, vol. 7, no. 2, pp. 212-223, May. 2011.

[25] O. Kaynak, K. Erbatur and M. Ertugnrl, "The fusion of computationally intelligent methodologies and sliding-mode control-a survey," in IEEE Transactions on Industrial Electronics, vol. 48, no. 1, pp. 4-17, Feb. 2001.

[26] V. Repecho, D. Biel and A. Arias, "Fixed Switching Period Discrete-Time Sliding-mode Current Control of a PMSM," in IEEE Transactions on Industrial Electronics, vol. 65, no. 3, pp. 2039-2048, March. 2018.

[27] W. Gao and J.C. Huang, "Variable structure control of nonlinear systems: A new reach," in IEEE Transactions on Power Electronics, vol. 40, no. 1, pp. 45-55, Feb. 1993.

[28] J. P. Mishra, X. Yu, M. Jalili and Y. Feng, "On fast terminal sliding-mode control design for higher order systems," IECON 2016 -42nd Annual Conference of the IEEE Industrial Electronics Society, Florence, 2016, pp. 252-257.

[29] Y. Zhang, Z. Yin, Y. Zhang, J. Liu and X. Tong, "A Novel Sliding Mode Observer With Optimized Constant Rate Reaching Law for Sensorless Control of Induction Motor," in IEEE Transactions on Industrial Electronics, vol. 67, no. 7, pp. 5867-5878, July. 2020

Yaoqiang Wang (M'16-SM'21) received his B.S. degree from Hangzhou Dianzi University, Hangzhou, China, in 2006; and his M.S. and Ph.D. degrees from the Harbin Institute of Technology, Harbin, China, in 2008 and 2013, respectively.

He is presently working in the School of Electrical Engineering, Zhengzhou University, Zhengzhou, China. He is also serving as the Director of the Institute of Power Electronics and Energy Systems of Zhengzhou University, the Zhengzhou Municipal Engineering Research Center of Power Control and Systems, and the Henan Provincial Engineering Research Center of Power Electronics and Energy Systems. He has published more than 50 peer-reviewed papers including over 40 journal papers, and is the holder of more than 10 patents. His current research interests include power electronics, renewable energy generation, flexible power distribution, MVDC, electric motor drives, and electrified transport.

Yachang Zhu received the B.S. degree in electrical engineering and its automation from the Henan University of Science and Technology, Luoyang, China, in 2017, and the M.S. degree in electrical engineering from Zhengzhou University, Zhengzhou, China, in 2021.

He is currently working as an Engineering Staff with the Yellow River Water Conservancy and Hydropower Development Group Co., Ltd, Zhengzhou 450001, China. His current research interests include power electronics and electric machine drives.

2332-7782 (c) 2021 IEEE. Personal use is permitted, but republication/redistribution requires IEEE permission. See http://www.ieee.org/publications_standards/publications/rights/index.html for more information.
Authorized licensed use limited to: Zhengzhou University. Downloaded on May 25,2021 at 15:13:45 UTC from IEEE Xplore. Restrictions apply.

This article has been accepted for publication in a future issue of this journal, but has not been fully edited. Content may change prior to final publication. Citation information: DOI 10.1109/TTE.2021.3083074, IEEE Transactions on Transportation Electrification

Xiaoguang Zhang (M'15-SM'21) received the B.S. degree in electrical engineering from the Heilongjiang Institute of Technology, Harbin, China, in 2007, and the M.S. and Ph.D. degrees in electrical engineering from the Harbin Institute of Technology, in 2009 and 2014, respectively. He is currently a Distinguished Professor at the North China University of Technology, and the director of Beijing Power Electronics and Electrical Transmission Engineering Research Center. From 2012 to 2013, he was a Research Associate at Wisconsin Electric Machines and Power Electronics Consortium (WEMPEC), University of Wisconsin–Madison, Madison. He has published more than 50 technical papers in the area of motor drives. He is serving as Associate Editor of IET Power Electronics. His current research interests include power electronics and electric machines drives.

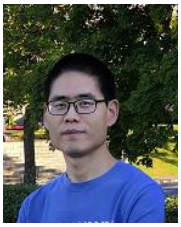

Bing Tian received the B.S. degree in electrical engineering and M.S. degree in control engineering both from Harbin Engineering University, Harbin, China, in 2011 and 2013, respectively; and Ph.D. degree in electrical engineering from Harbin Institute of Technology, Harbin, China, in 2018. From 2018 to 2020, He was a postdoctoral research fellow with Norwegian University of Science and Technology (NTNU), Trondheim, Norway, working on the electrification of offshore production system in close collaboration with Norwegian industry. Since September 2020, he has been a Research Associate Professor with the department of electrical engineering of Nanjing University of Aeronautics and Astronautics (NUAA), Nanjing, China. His current research interests include fault-tolerant control of multi-phase drives, sensorless control of electric drives, neural network, sliding mode controller/observer, and repetitive control.

Kewen Wang received his B.S. degree from the Zhengzhou Institute of Technology, Zhengzhou, China, in 1985; his M.S. degree from Tianjin University, Tianjin, China, in 1988; and his Ph.D. degree from Hong Kong Polytechnic University, Hong Kong, China, in 2000.

He is currently a Professor with the School of Electrical Engineering, Zhengzhou University, Zhengzhou, China. His research interests include power electronics, renewable power generation, power system stability analysis and control, reactive power optimization.

Jun Liang (M'02-SM'12) received his B.S. degree in Electric Power System & its Automation from the Huazhong University of Science and Technology, Wuhan, China, in 1992; and his M.S. and Ph.D. degrees in Electric Power System & its Automation from the China Electric Power Research Institute (CEPRI), Beijing, in 1995 and 1998, respectively.

From 1998 to 2001, he was a Senior Engineer with CEPRI. From 2001 to 2005, he was a Research Associate with Impe-rial College London, U.K. From 2005 to 2007, he was with the University of Glamorgan as a Senior Lecturer. He is currently a Professor in Power Electronics with the School of Engineering, Cardiff University, Cardiff, U.K. He is the Co-ordinator and Scientist-in-Charge of two European Commission Marie-Curie Action ITN/ETN projects: MEDOW (€3.9M) and InnoDC (€3.9M). His research interests include HVDC, MVDC, FACTS, power system stability control, power electronics, and renewable power generation.

Prof. Liang is a Fellow of the Institution of Engineering and Technology (IET). He is the Chair of IEEE UK and Ireland Power Electronics Chapter. He is an Editorial Board Member of CSEE JPES. He is an Editor of the IEEE Transactions on Sustainable Energy.

2332-7782 (c) 2021 IEEE. Personal use is permitted, but republication/redistribution requires IEEE permission. See http://www.ieee.org/publications_standards/publications/rights/index.html for more information.
Authorized licensed use limited to: Zhengzhou University. Downloaded on May 25,2021 at 15:13:45 UTC from IEEE Xplore. Restrictions apply.